




Article

Accelerating CO₂ Storage Site Characterization through a New Understanding of Favorable Formation Properties and the Impact of Core-Scale Heterogeneities

Chidera O. Ilojesi , Will Beattie, Frances C. O'Donnell  and Lauren E. Beckingham * 

Department of Civil and Environmental Engineering, Auburn University, Auburn, AL 36849, USA; coi0002@auburn.edu (C.O.I.); wab0030@auburn.edu (W.B.); fco0002@auburn.edu (F.C.O.)

* Correspondence: leb0071@auburn.edu; Tel.: +1-334-844-6260

Abstract: CO₂ sequestration in deep geologic formations can permanently reduce atmospheric CO₂ emissions and help to abate climate change. Target formations must undergo a time- and resource-intensive site evaluation process, assessing storage capacity, environmental safety, and suitability for CO₂ trapping via reactive transport models based on data from a limited number of core samples. As such, simulations are often simplified and omit heterogeneities in formation properties that may be significant but are not well understood. To facilitate more rapid site assessment, this work first defines the aquifer properties of favorable storage formations through the analysis of promising and active storage sites. Data show quartz is the most prevalent formation mineral with carbonate minerals, highly reactive with injected CO₂, present in over 75% of formations. Porosity and permeability data are highly clustered at 10–30% and 10–1000 mD. Field-scale reactive transport simulations are then constructed and used to analyze CO₂ trapping efficiency. The models consider porosity and carbonate mineral heterogeneity as well as the impacts of typical temperature gradients. Simulated sequestration efficiencies are compared to results from a comparable homogenous model to understand the implications of aquifer non-uniformities. The results show a lower sequestration efficiency in the homogeneous model during the injection phase. During the post-injection phase, the homogenization of porosity and carbonate mineralogy results in a higher sequestration efficiency. Incorporating the temperature gradient also increases the sequestration efficiency. Importantly, the maximum deviation between the homogeneous and heterogeneous simulations at the end of the 50-year study period is only ~10%. Larger impacts may be incurred for properties outside the defined, promising ranges suggested here.

Keywords: carbon sequestration; aquifer properties; reservoir heterogeneity; site investigation; CO₂ mitigation; reactive transport modeling



Citation: Ilojesi, C.O.; Beattie, W.; O'Donnell, F.C.; Beckingham, L.E. Accelerating CO₂ Storage Site Characterization through a New Understanding of Favorable Formation Properties and the Impact of Core-Scale Heterogeneities. *Sustainability* **2024**, *16*, 5515. <https://doi.org/10.3390/su16135515>

Academic Editor: Mohammad Aslam Khan Khalil

Received: 21 May 2024
Revised: 11 June 2024
Accepted: 21 June 2024
Published: 28 June 2024



Copyright: © 2024 by the authors. Licensee MDPI, Basel, Switzerland. This article is an open access article distributed under the terms and conditions of the Creative Commons Attribution (CC BY) license (<https://creativecommons.org/licenses/by/4.0/>).

1. Introduction

While renewable energy generation is increasing [1], energy demands necessitate continued energy production through hydrocarbons [2]. Unfortunately, CO₂ emissions, a major greenhouse gas and contributor to climate change, continue to increase as a consequence of fossil fuel use [3,4]. Carbon capture and geologic storage, however, provides a pathway for reducing atmospheric CO₂ emissions and can aid efforts to achieve future energy sustainability and net-zero carbon emissions [5]. This technology averts the release of CO₂ into the atmosphere by capturing it and then injecting the CO₂ into subsurface geologic formations [6]. Large-scale and widespread application of this technology will involve the utilization of porous saline aquifers as storage reservoirs due to their ubiquity and enormous available storage volume [7,8].

The Class VI injection well permit issued by the U.S. Environmental Protection Agency (EPA) for the geologic sequestration of CO₂ is based on the requirement for safe injection and storage. Therefore, the storage aquifer is expected to be geologically stable against

potential tectonic activities, porous, permeable, sufficiently deep, and sealed by impermeable rocks or caprocks [9]. There are myriads of potential considerations to guarantee the success of the project each time the subsurface is utilized for the development of CO₂ sequestration technology. A thorough subsurface site investigation is carried out before developing a project to ensure potential storage aquifers meet these guidelines and to guarantee the success of the project and the onsite safety [8,10,11]. This is a time- and resource-intensive process and may inhibit the widespread adaptation of such approach. Existing site data may be limited, and additional site sampling is often restricted to a few select wells. As such, the suite of geological wellbore log information and core sample data used for estimating and evaluating the storage capacity and response of the entire formation to CO₂ injection is estimated from select points in the formation. Nevertheless, the borehole logging, geophysical mapping, core sample analysis, well testing, and geological mapping from these select spots still provide meaningful overall insights into the suitability of the target formation to store CO₂.

Numerical modeling can be used to provide rapid insight into the field-scale geochemical behavior of CO₂ injected into the subsurface and assess the potential viability of new storage sites [12–14]. Numerical simulations have been used to study the complexity of various subsurface conditions that affect CO₂ storage and consider trapping rates and mechanisms, often validated with laboratory experimental observations [15]. In other cases, numerical modeling has been used independently to understand the potential geochemical evolution of a storage site, comparing results to field observations [10,16]. Models can provide invaluable information of the geochemical suitability of a formation for CO₂ storage where an ideal site promotes the secure trapping of injected CO₂. This includes trapping of the injected CO₂ by the caprock, termed structural trapping, dissolution of CO₂ in the brine (solubility trapping), residual trapping of free phase CO₂ bubbles, and mineralization [17,18]. Mineralization is the conversion of CO₂ to carbonate rocks that permanently sequester the CO₂. This is the most secure and favorable form of trapping and highly desirable sites favor mineralization of the injected CO₂ [19,20].

While powerful, numerical simulations are often based on the available limited site data, requiring the simplification of site geology and aquifer properties. In reality, aquifer properties may be spatially heterogeneous [21], resulting from the diagenetic evolution of the original sediment [22]. Larger-scale lithological heterogeneities, resulting from variations in facies [23] or the presence of faults [24], may also exist.

Heterogeneities in aquifer properties can impact fluid flow [25,26], the migration of CO₂ [27], and CO₂–brine interactions [28,29]. Prior work has noted that large-scale stratigraphic heterogeneities control the migration of the CO₂ plume and need to be accurately parameterized. For example, siltstone rock layering over a sandstone reservoir has been shown to limit plume migration and promote geochemical conditions encouraging the extensive reaction and mineralization of the injected CO₂ [30]. There have also been attempts to examine the impacts from the heterogeneity of hydrologic and geochemical properties on CO₂ sequestration. Using the Mt. Simon formation as a case study, simulations from Shabani et al. (2022) [31] showed that considering the heterogeneity of porosity and permeability impacted CO₂–water–mineral interactions where the migration of the CO₂ plume was restricted in heterogeneous systems, resulting in more extensive CO₂ mineral trapping and a higher likelihood of long-term containment. In terms of geochemical reactions, the spatial heterogeneity of caprock mineralogy has been suggested to improve the long-term sealing capacity of caprocks [32]. While these case studies suggest that heterogeneity is important in understanding the fate of injected CO₂, a fundamental understanding of the impacts of aquifer property heterogeneity on the geochemical evolution of injected CO₂, that could help to facilitate more rapid site assessment is lacking. Developing this conceptual understanding through a systematic evaluation of aquifer property heterogeneity is the focus of this work.

In this work, a framework for more rapid site assessment in terms of trapping potential is considered. First, a thorough evaluation of the acceptable range of formation properties is

gained by surveying data from active and promising storage formations. These data alone provide an initial means of site screening that can help to rapidly identify formations of interest. Then, reactive transport simulations are leveraged to assess the need to carry out an extensive, core-scale characterization of the heterogeneities in the formation properties. Simulations consider the geochemical implications of heterogeneous distributions of aquifer porosity, formation depth, and carbonate composition. This study is unique in not only providing a comprehensive survey of promising formation properties, but additionally considering the mineralogy of the formations and the impact of accounting for heterogeneous mineralogy at the core to field scale on CO₂ trapping.

The Paluxy sandstone formation, southeastern United States, is considered as a case-study, and heterogeneity is introduced by considering the range of formation properties from aquifers identified as promising or operational storage formations. CO₂ trapping in homogenous and heterogeneous formations is evaluated via field-scale reactive transport simulations. Spatial heterogeneities in porosity and carbonate mineralogy are considered in addition to simulations incorporating and excluding temperature gradients. The simulation results are analyzed to understand how the heterogeneity associated with temperature, porosity, and carbonate mineralogical composition impact simulate sequestration efficiency and thus the assessment of potential sequestration sites. Sequestration efficiency refers to the rate at which the injected supercritical CO₂ evolves to be dissolved into the formation brine or mineralized as carbonate minerals.

2. Evaluating Aquifer Properties

A systematic literature review was conducted to gather data on the characteristics of sandstone saline aquifers identified as promising or operational storage reservoirs. Data collection was streamlined to consider only actual site investigations for aquifers that are currently being used for CO₂ storage or evaluated as a potential storage site and exclude data points that are hypothetical estimates. The associated promising formations include CO₂ storage projects in sandstone aquifers from around the world which are completed, under consideration, or terminated (for economic or legal reasons [33]). The data of interest here include mineral composition, fraction of carbonate minerals, reservoir porosity, permeability, thickness, and depth. These data are important in understanding the suitability of a target aquifer and the associated favorable property values which can serve as a quick resource for rapid initial evaluation of the promise of a particular storage aquifer.

Aquifer mineral composition is important for considering the potential long-term security of carbon sequestration in geological formations. Geochemical reactions that dissolve primary formation minerals are an important source of cations that promote secure mineral trapping. Such reactions may alter the storage capacity and injectivity of the formation by changing the formation porosity and permeability [34]. Carbonate minerals in particular have been observed to rapidly react upon interaction with the acidified brine and are thus critical in assessing the associated impacts on the formation properties [35,36].

The total available volume for carbon storage is a function of the total available pore volume of a reservoir. Thickness has a direct relationship with the total available pore volume, indicating that a thicker formation will have more available volume for carbon storage [37]. Hence, due to the significant capital investments associated with establishing a carbon storage operation at a potential reservoir, higher storage capacities result in lower unit prices for carbon storage at a target location [35,36].

Reservoir depth is also an important parameter for the selection of a promising storage reservoir. At sufficient depths, storage reservoirs achieve pressures large enough to maintain CO₂ in the supercritical phase. In the supercritical state, the density of CO₂ is substantially larger, facilitating an increased storage capacity. CO₂ solubility is additionally enhanced under such conditions. Hence, reservoir depth can influence the security of CO₂ storage. However, it is worth noting that for a greenfield site, carbon storage costs generally increase as injection depth increases due to the exploration costs of drilling [35,36].

The complete data set of the collected aquifer properties is available in Table S1. The collected data include twenty-nine different sandstone formations from four continents. The relative frequency of formation mineralogy is shown in Figure 1 and indicates that quartz is the most prevalent formation mineral in the associated formations followed by feldspar, clay, and carbonate minerals. All target sandstone formations contain, and are predominantly composed of, quartz. As such, Figure 1 shows that the relative frequency of quartz is unity and the relative weight percentage of quartz ranges from 30% to 95% with an average abundance of over 75%. Feldspar minerals are highly ubiquitous and their interquartile range is relatively typical to the other minerals in the formation. Calcite is the most prevalent carbonate mineral noted in the storage formations followed by dolomite while ankerite is the least frequent carbonate mineral. However, ankerite possesses the highest average abundance. Clay minerals are commonly kaolinite or smectite/illite. It is worth noting that this reflects only the initial mineralogy and that other mineral phases may precipitate because of geochemical reactivity which is not accounted for in Figure 1.

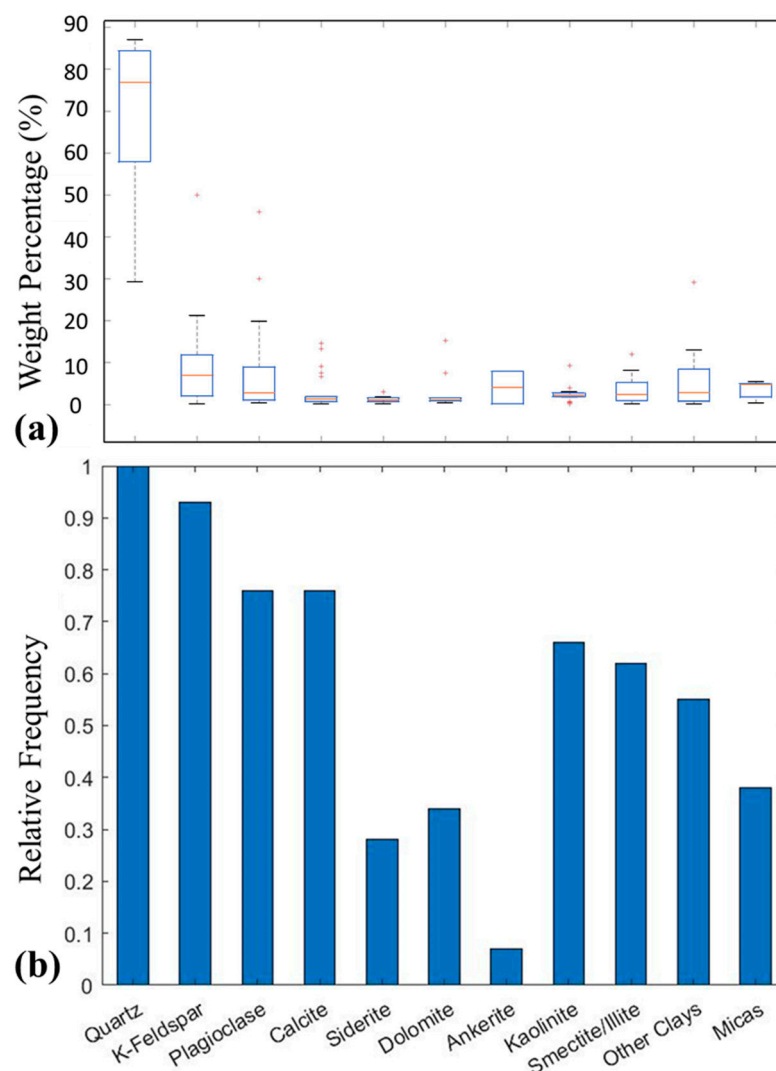


Figure 1. Box plot of the relative mineral weight percentage in a rock matrix (a) and the relative frequency plot of initial mineral composition of potential and operational sandstone storage formations (b).

The distributions of formation porosity, permeability, aquifer depth, and thickness are shown in Figure 2. The porosity and permeability values range from 3% to 43% porosity (Figure 2a) and 0.08 mD to 5000 mD permeability (Figure 2b). The permeability distribution

has a large frequency of low permeabilities (0.08–456 mD). Overall, the permeability has a logarithmic distribution with sparse data in the higher permeability values. The distribution of the porosity data is not sparse at either boundary but there are a few formations with porosity values at the high and low extremes which results in a right skewed distribution. Many formations have porosity values between 10% and 20% with the frequency consistently decreasing with increasing porosity values.

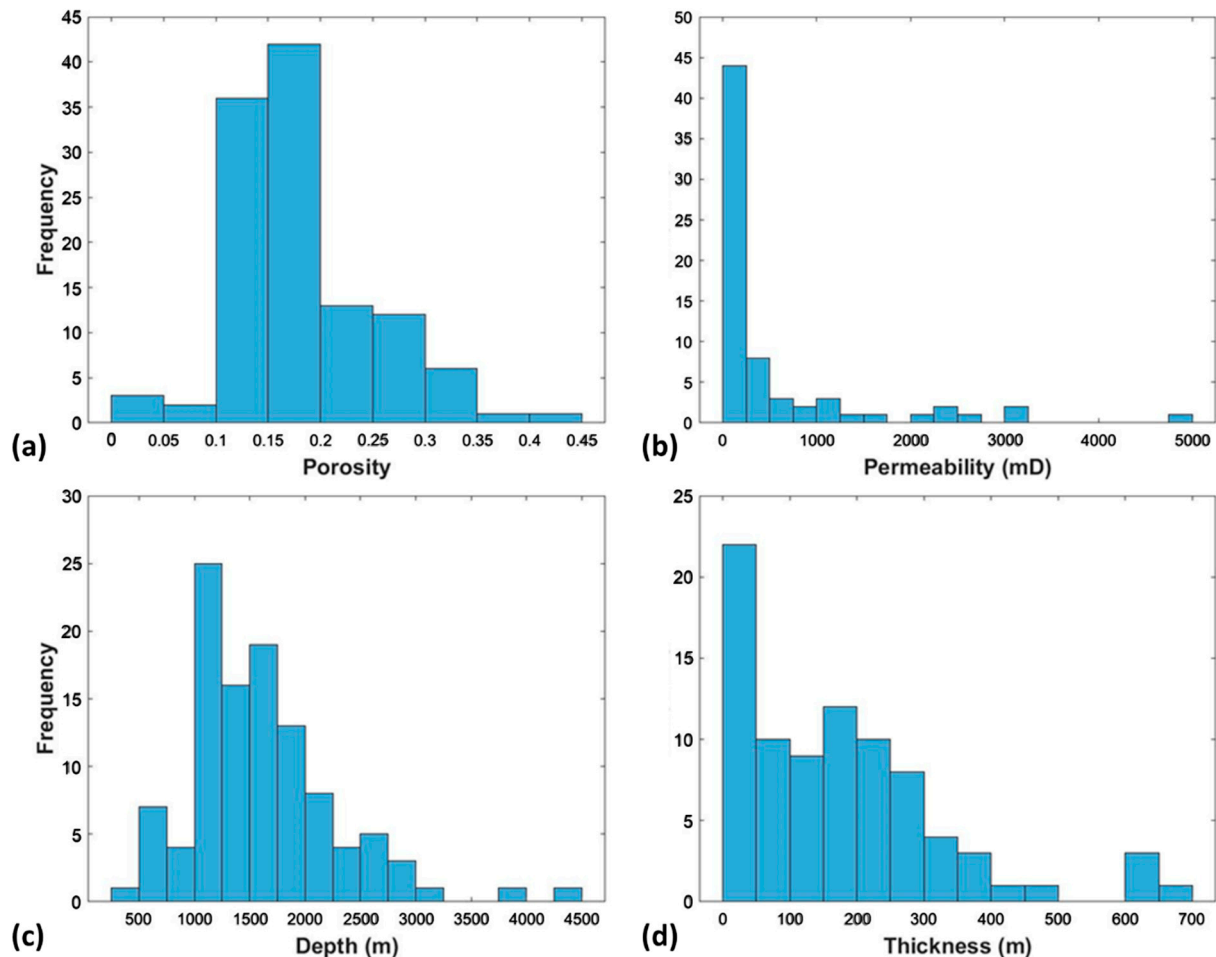


Figure 2. The frequency distribution of (a) porosity, (b) permeability, (c) depth, and (d) thickness of a sandstone storage aquifer.

The distribution plots of aquifer depth and thickness show maximum values of 4500 m and 700 m, respectively (Figure 2d). Like the permeability distribution, the thickness data points are sparse and few at the upper limits (Figure 2c). The distribution of thickness is logarithmic since the majority of formations have thickness values that are closer to the minimum thickness. In terms of the depth distribution, there is an outlying deeper formation depth which, when ignored, makes the mean and median depth of storage approximately 1500 m. It should be noted that given the typical geologic temperature and pressure gradients, depths beyond ~800 m result in conditions for CO₂ to exist in the supercritical state, facilitating higher storage capacities. Temperature and pressure conditions vary with location such that shallower formations, like the Stuttgart and Bunter formations, may also meet the criteria for CO₂ to be stored in the supercritical phase [21,38].

The collected paired porosity–permeability values are shown in Figure 3 and cover a wide range of values, both between and within formations where in-formation variability is indicated by the permeability error bars. The majority of data points are in the 10–30% porosity range with a corresponding 10–1000 mD permeability, defining the typical characteristics of promising CO₂ storage aquifers. Sufficient porosity–permeability is necessary to

ensure adequate storage capacity and injectivity. Higher porosity and permeability present more favorable injection qualities such as a better pressure dissipation during injection. Porosity and permeability values lower than the typical range may still be favorable for CO₂ sequestration where additional features, such as natural fractures, may allow for sufficient flow in the formation [38]. Geochemical reactions following CO₂ injection, including the dissolution of primary mineral phases, may also increase the porosity and permeability of the formation, enhancing injectivity [39]. Maintaining sufficient CO₂ injectivity while ensuring the storage aquifer is adequate for storing the injected fluid is one of the key concerns when accessing the porosity and permeability of a potential storage aquifer [40,41]. Such geochemical effects are considered in the following reactive transport simulations.

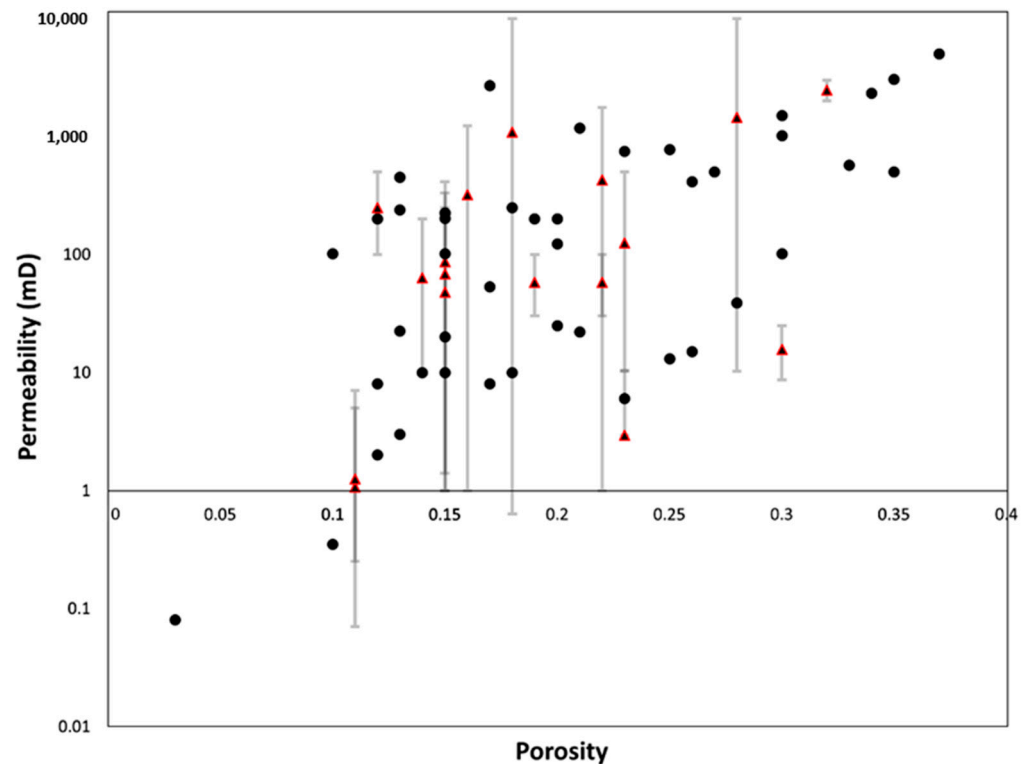


Figure 3. Porosity–permeability plot for sandstone aquifer CO₂ storage reservoirs. The black dots represent formations with a single data point for a given aquifer and the error bar represents the range of values for cases for which there are numerous available data points available for a given formation with the mean values indicated by the red triangle.

3. Reactive Transport Model

The simulation approach adopted here aims to help us to understand the effects of aquifer property heterogeneity on CO₂ sequestration efficiency. A finite number of wells, and associated samples extracted from corresponding wells, are examined during the site investigation process. As this is a time- and resource-intensive process, and the creation of additional wells may also introduce additional leakage pathways, only a finite number of data points are available from which to carry out detailed reactive transport simulations to assess the engineering design and the large-scale, long-term impacts of CO₂ sequestration in a particular formation. As such, simulations often utilize average formation parameters based on a single or finite number of measurements to define the aquifer. However, such properties may widely vary at the core to field scale, as is evident for the permeability measurements in Figure 3. As such, the implications of this practical limitation from a CO₂ trapping perspective are considered through two sets of field-scale simulations, one with homogeneously distributed properties and the other with spatially heterogeneous distributions of aquifer properties. To compare the impact of spatial heterogeneity on

the site evolution, the average properties for the two sets of simulations are equivalent. Noted heterogeneities in properties may or may not be well-characterized in the formation, even after an excellent site investigation study has been carried out. Moreover, accounting for such core- to field-scale heterogeneity in simulations significantly increases the model complexity and may not be numerically feasible. As such, most simulation studies adopt initial conditions that seem to be more suited for the local evaluation of an aquifer, versus field scale.

The field-scale modeling work here builds off the of the TOUGHREACT reactive transport simulator model developed in Ilojesi et al. (2023) [29]. The simulator couples subsurface multiphase transport and reaction and uses the ECO2N fluid property module to handle the CO₂ and water thermophysical properties under the typical range of temperature and pressure conditions of a saline aquifer [42,43]. A radially symmetric two-dimensional model is used here to consider the extent of CO₂ trapping in porous saline aquifers. The aquifer was discretized into 20 layers using a uniform and logarithmically increasing radial discretization with the lateral boundary considered to be at infinity to mimic constant temperature, concentration, and pressure conditions at the boundaries.

Two sets of models were developed for this study. The first set, a homogeneous model, was initialized with the aquifer properties of the Paluxy formation located in the southeastern region of the United States which is being considered as a potential CO₂ storage formation [44–46]. The second set, the heterogeneous models, were initialized with spatial variations in aquifer properties, aiming to evaluate the impact of each property on the sequestration efficiency of injected CO₂ independently.

The parameters for the homogenous and heterogenous simulations are given in Table 1. The rest of the model is defined via the properties of the Paluxy formation as obtained from the literature and given in Table S4 [45]. This formation is predominantly quartz (76.74 w%) with over 10% carbonate minerals (9.70 w% calcite and 2.98773 w% siderite), 7.19 w% smectite, and minor K-feldspar (3.33 w%) and muscovite (0.32 w%). This is a typical mineralogic composition in comparison to other favorable storage formations (Figure 1). Also, in comparison to the other studied aquifer properties of the storage formation, the 25% porosity, 500 mD permeability, and 1500 m depth of storage of the Paluxy formation are slightly higher than the modal values of 18% porosity, 100 mD permeability, and 1400 m depth observed for a typical aquifer in the literature review. Tables S4 and S5 have more information on the model parameters including mineral composition, reactive surface areas, hydrostatic pressure gradient, and temperature. The hydrostatic pressure gradient of 0.43 psi/ft was used [47] and the temperature was calculated based on the surface temperature of 20 °C and temperature gradient of 20 °C/km [48,49].

Spatial heterogeneity was defined in the heterogenous simulations by randomly assigning aquifer properties to the model grid cells, ensuring the average initial value of the entire grid matched the property value assigned to the entire grid for the homogeneous model. For example, in the model that considered porosity heterogeneity, five different porosities ranging from 10% to 40% were randomly assigned to the aquifer grid (Figure S1) while maintaining the overall average porosity of the entire grid as 25% which was equivalent to the porosity of the Paluxy formation used to define the homogeneous model. Similarly, the model for evaluating the impact of carbonate mineral heterogeneity in the rock matrix considered five different values for carbonate abundance with equal proportions of siderite and carbonate. These mineral abundances were randomly assigned to grid cells to maintain an average carbonate mineral abundance equivalent to the homogeneous system. The quartz fraction was adjusted to accommodate the variation in the fraction of carbonate minerals in associated simulations as quartz has been shown to minimally affect geochemical reactions because of its slow kinetics and stability in acidic conditions [50]. Lastly, a non-isothermal model setup with a geothermal gradient of 20 °C/km was used to depict the subsurface temperature variation in a heterogeneous model. A constant temperature of 50 °C, corresponding to the temperature at the center of the aquifer thickness, was used to initialize the isothermal model for the corresponding homogeneous simulation.

Table 1. Simulation parameter values for each considered aquifer property. Aquifer formation properties for acting and proposed CO₂ reservoir formations were collected from the literature. The values are representative of the range of aquifer properties in these target formations and do not necessarily correspond to the exact values. The heterogenous values are chosen so that the aquifer value could be numerically the average of the homogeneous model.

Model Setup		Porosity	Carbonate Content (wt%)	Temperature (Associated Depth)
Heterogeneous model	Case 1	10%	2%	49.6 °C (1500 m) through 50.4 °C (1540 m)
	Case 2	20%	5%	
	Case 3	25%	12.5%	
	Case 4	30%	16%	
	Case 5	40%	21%	
Homogeneous model		25%	12.5%	50 °C (1520 m)

Both homogenous and heterogenous models considered a single CO₂ injection well with an eight-meter injection screen thickness. The two-dimensional evolution of the injected CO₂ phase used the van Genuchten function for capillary pressure and the van Genuchten–Mualem model for water relative permeability, respectively [51,52]. The gas relative permeability for the two-phase system was modeled with Corey’s curve [53]. The activity of aqueous species was modeled using the extended Debye–Huckle equation [54,55]. The initial brine composition was determined via equilibration of the formation minerals with 1M NaCl brine [13].

Simulations considered constant CO₂ injection at a 20 kg/s injection rate for ten years followed by geochemical monitoring for forty years, reflecting anticipated typical required short-term monitoring periods [56]. This simulation period provides useful information for understanding CO₂ stratigraphic, solubility, and mineral trapping for reservoirs with varied properties. It should be noted, however, that mineral trapping continues over extended time periods with previous studies considering 500 to 1000-year monitoring periods showing that the amount of mineralized CO₂ increases close to linearly with time [57]. As in Ilojesi et al. (2023) [29], we track the relative quantity of the aqueous, supercritical, and mineralized CO₂ in the system (further details in Supplementary Materials).

4. Simulation Results

The simulation results compare the evolution of supercritical, dissolved, mineralized, and trapped CO₂ in the homogeneous and heterogeneous models for each case of heterogeneity. The term trapped CO₂ is used here to refer to the summation of the amount of aqueous and mineralized CO₂. The sequestration efficiency, the amount of injected CO₂ that evolves from supercritical CO₂ to aqueous and mineralized CO₂, is calculated and compared for each simulation.

4.1. Varied Carbonate Mineral Fraction

The effect of spatial variations in the carbonate mineral fraction on the simulated evolution of injected CO₂ is shown in Figure 4. The simulation results depict the CO₂ in varied phases across the entire simulation domain. Differences in these simulations consider only grid-scale differences in the fraction of carbonate minerals while keeping the other aquifer properties equal to those of the homogeneous model. The simulation results show that the rate at which the injected CO₂ evolves into aqueous and mineralized CO₂ is greater during the injection phase for the heterogeneous system compared to the homogeneous system. As the reactions progress, the rate of aqueous dissolution and mineralization of CO₂ in the system becomes greater in the homogeneous model. The dissolution rate of CO₂ into the aqueous phase notably increases in the homogenous system following injection

with the total mass of dissolved CO₂ surpassing that in the heterogenous simulation after 15 years.

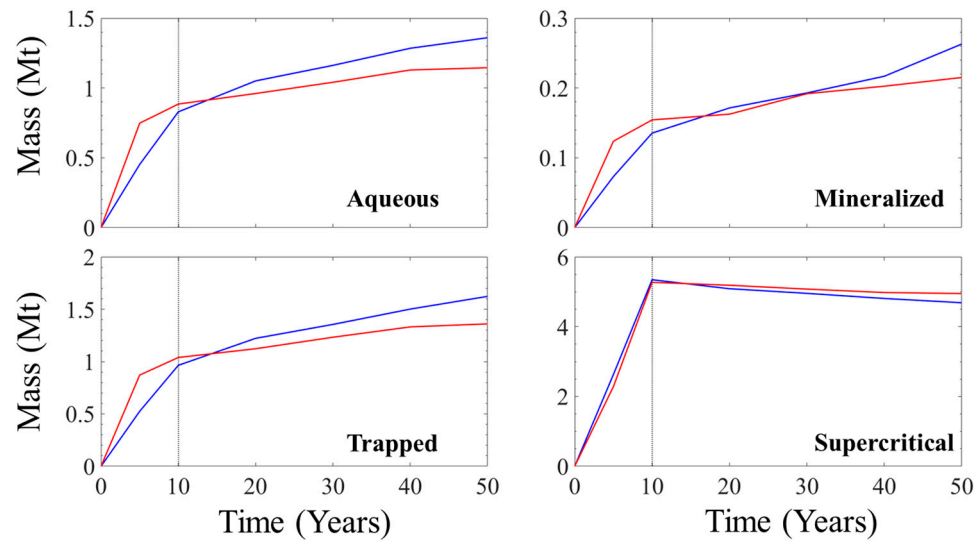


Figure 4. Comparison of the simulated aqueous, mineralized, trapped, and supercritical CO₂ in millions of metric tons over 50 years for simulations with varying carbonate mineral fractions. The dashed vertical line signals the end of the injection period, the red line the results from the simulation including a heterogenous distribution of carbonate minerals, and the blue line the simulation results from the model with a homogeneous carbonate mineral content.

The trapped CO₂, which combines the evolution of aqueous and mineralized CO₂, shows that a formation with a heterogeneous distribution of carbonate minerals results in a higher mass of sequestered CO₂ in the early stages of the injection and storage phase, before 15 years. Over longer times, however, the homogenous system performs better in terms of lowering the amount of free, supercritical CO₂ over the simulation duration by just over 0.2 million tons. This observed difference at 50 years is largely a result of the increased aqueous dissolution of CO₂ in the homogenous model. Carbonate minerals in contact with acidified brine undergo relatively fast dissolution which increases formation porosity and liberates divalent cations that promote mineralization [58,59]. The increase in pore volume increases the brine volume available for the dissolution of supercritical CO₂ into the aqueous phase. This increased dissolution of CO₂ into the aqueous phases reduces the solution pH, further promoting the dissolution of carbonate minerals. The increase in divalent cations that results from increased mineral dissolution creates conditions more favorable for the mineralization of CO₂.

To understand the difference in the impact of carbonate on the homogenous and heterogenous systems, it should be noted that the dissolution of carbonate minerals releases carbonate ions into solution. As such, the reprecipitation of new carbonate minerals may not be sequestering the CO₂ that was injected into the formation but instead incorporating carbonate ions released from primary minerals. Sequestration of the injected CO₂ via mineralization occurs when the cations incorporated into new carbonate mineral precipitates originate from non-carbonate minerals. Both such processes may occur here, but it is not feasible to discern from where the carbonate ions incorporated into newly precipitated carbonate minerals originate.

The heterogeneous model has cells with as high as 35 w% carbonate minerals. Regions with higher fractions of carbonate minerals are highly reactive zones that favor mineral dissolution, liberating more positive divalent cations like calcium, magnesium, and iron which favor subsequent secondary mineral precipitation. This is evident in the higher simulated early aqueous and mineral trapping in the heterogenous model over the homogenous model. However, more rapid dissolution of the primary carbonate minerals

reduces the overall fraction of carbonate minerals in the system, eventually resulting in the homogenous model having more remaining high-carbonate grid cells in the domain. This is the point when the observed transition in the amount of mineralized CO₂ begins to favor the homogeneous system.

It should be noted that the kinetics of mineral reactions are important and significantly slower than the transport-controlled process of aqueous dissolution. Hence, the simulation result of Figure 4 shows that unlike in the aqueous CO₂ evolution graph where the rate of aqueous dissolution changed instantaneously after 15 years from a heterogeneous system to a higher value in the homogeneous system, the transition to a higher mineralization rate of the homogeneous model happened over a prolonged period that spanned from 20 years to 30 years for the mineralization evolution. The associated time for mineralization to occur in a particular storage site will depend on the unique kinetic and geochemical properties that characterize the formation. As such, the timescale for the observed evolution in mineralized CO₂ between the homogenous and heterogenous simulations will be site dependent.

4.2. Porosity Heterogeneity

The simulated evolutions of aqueous, mineralized, trapped, and supercritical CO₂ for simulations with homogenous and heterogeneous distributions of porosity are shown in Figure 5. The only difference between the two simulations is the variation in the initial porosity values of individual grid cells. During the injection phase (the first 10 years), a higher extent of CO₂ dissolution into the aqueous phase is evident for the heterogeneous simulation. At the end of the injection phase, however, the mass of aqueous CO₂ in both simulations is about equal (Figure 5). From that point on, the mass of aqueous CO₂ in the homogeneous model is greater, and increases at a higher rate, than in the heterogeneous model. The extent of mineralized CO₂ is higher in the heterogeneous system than the homogenous system for the duration of the simulation period. The simulated trapped CO₂ shows that initially CO₂ trapping via dissolution and mineralization is higher in the heterogeneous model than the homogeneous model throughout the injection phase and for the initial monitoring years. As the mineralization rate and the aqueous dissolution rate decrease in the heterogeneous model, the trapped CO₂ increases in the homogeneous model, eventually surpassing that of the heterogenous model. As a result, there is less free supercritical CO₂ in the homogeneous model at the end of the study period.

The variation in porosity in the heterogenous model introduces a range of water-to-rock ratios in the simulation which highlights the difference in the storage efficacy between the homogeneous and heterogeneous system. In cells with small water-to-rock ratios, reduced extents of mineral dissolution are required to reach ion concentrations favoring mineral precipitation. Hence, the observed initial high rate of mineralization in the heterogeneous model is attributed to the faster mineral precipitation occurring in the low porosity grid cells of the heterogeneous model. Larger water-to-rock ratios provide an increased driving force for dissolution and associated increased brine capacity to accommodate more supercritical CO₂ dissolution into the aqueous phase. We see here that the aqueous CO₂ was marginally higher in the heterogeneous model during the injection period. Initially, the low-porosity grid cells are the drivers of the mineral reactivity that favor higher mineralization in the heterogeneous model. Over time, the dominating reactive regions in the heterogeneous model will be the high-porosity grid cells in which porosity was as much as 15% more than the initial porosity of the homogeneous model cells.

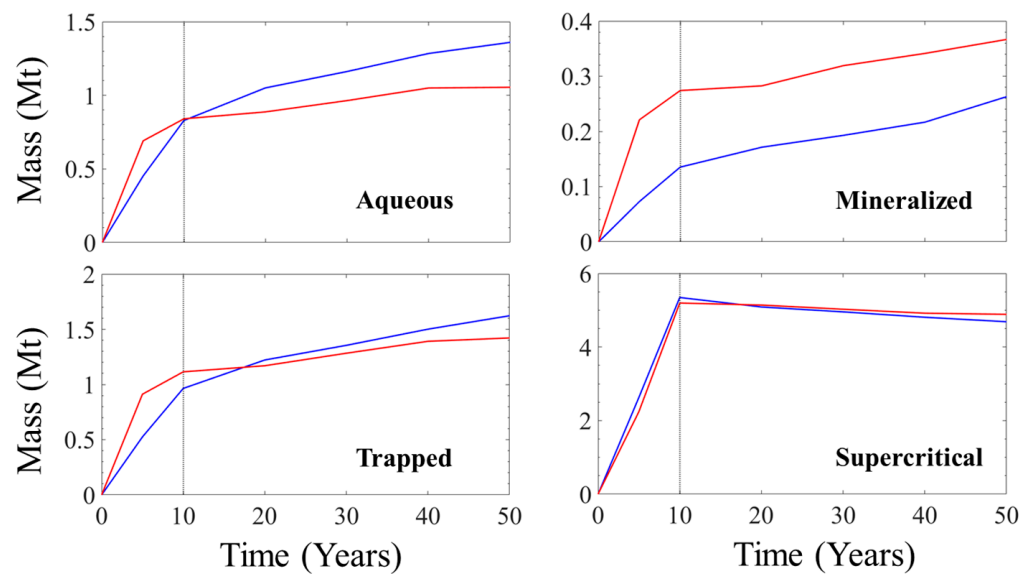


Figure 5. Comparison of the simulated aqueous, mineralized, trapped, and supercritical CO₂ in millions of metric tons over 50 years for simulations with varying porosity distribution. The dashed vertical line signals the end of the injection period, the red line the results from the simulation including a heterogenous distribution of porosity, and the blue line the simulation results from the model with homogeneous porosity.

4.3. Effect of Temperature Gradient

The homogenous simulation in this case uses a uniform temperature throughout the domain, while the heterogeneous model considers a typical vertical temperature gradient of 20 °C/km. CO₂ injection is simulated into the deepest part of the domain, corresponding to the highest-temperature region in the heterogeneous model.

The simulation results (Figure 6) show a similar trend in the behavior of the aqueous and mineralized CO₂ for the homogenous and heterogenous simulation with a higher rate of conversion of the injected CO₂ to the aqueous and mineralized form in the heterogeneous model during injection. Here, higher temperatures also increase mineral reaction rates and higher rates of mineralization are evident in the heterogeneous simulation results. Consequently, the resulting trapped CO₂ shows that overall, more CO₂ is in the aqueous and mineralized form in the heterogeneous model. As such, there is a lower amount of supercritical CO₂ in the heterogeneous model than in the homogeneous model for the whole study period.

While overall, the homogeneous and heterogeneous models have an equal average aquifer temperature, the storage impacting difference lies in the inclusion of the temperature gradient which has a noticeable impact on the simulation results. This difference caused by temperature heterogeneity shows that a poor understanding of aquifer temperature conditions could lead to remarkable distortions of the simulated CO₂ sequestration efficiency at a storage site. This is because temperature plays a key role in the kinetics of the geochemical reactions.

4.4. Assessment of Aquifer Properties Importance on Heterogeneity

A comparison of the simulated trapped CO₂ for the homogenous and heterogenous simulations over varying times is shown in Figure 7 by considering the difference between the trapped CO₂ in the heterogeneous models and the homogeneous model. A positive value of trapped CO₂ mass signifies a higher mass of trapped CO₂ in the heterogeneous model. The figure shows that the homogenization of aquifer properties will yield a lower simulated estimate of the mass of trapped CO₂ during the injection phase (0–10 years). Post-injection, assuming a uniform porosity and carbonate mineral fraction throughout the formation results in greater simulated CO₂ trapping. However, using a

single temperature for the formation, and ignoring the expected temperature gradient in the formation, underestimates the potential extent of CO₂ trapping throughout the injection and monitoring period.

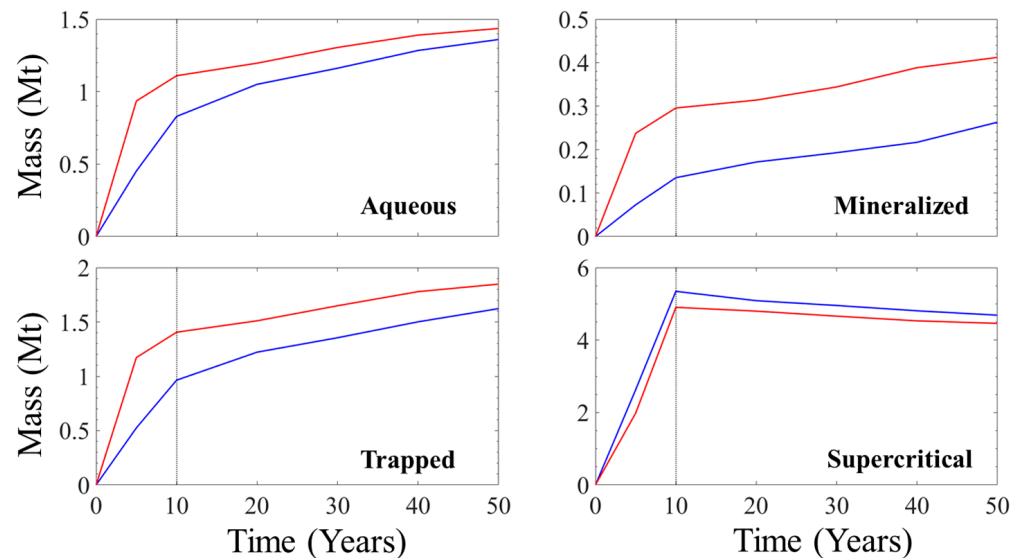


Figure 6. Comparison of the simulated aqueous, mineralized, trapped, and supercritical CO₂ in millions of metric tons over 50 years for simulations with temperature variation with depth. The dashed vertical line signals the end of the injection period, the red line the results from the simulation including the temperature gradient, and the blue line simulation results from the homogeneous model.

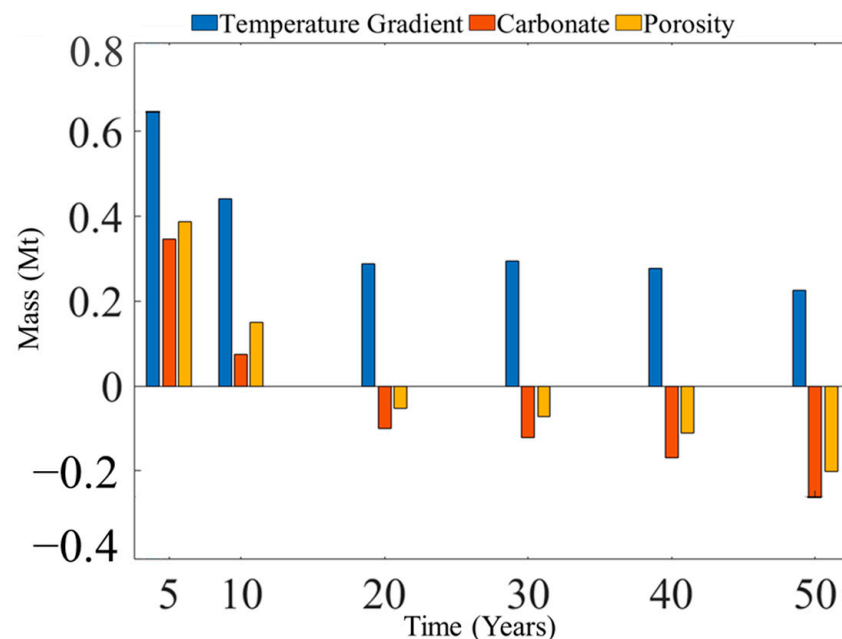


Figure 7. Simulated mass comparison in millions of metric tons of the difference between the trapped CO₂ in the heterogeneous and homogeneous models. The blue, orange, and yellow represent the temperature, carbonate, and porosity, respectively. A bar with a value of 0.2 Mt means that the difference in trapped CO₂ for the homogeneous and heterogeneous models is 0.2 Mt.

Capturing small-scale variations in porosity and carbonate mineralogy is relatively impractical due to time, resource, and risk limitations. On the other hand, it is easy to account for temperature gradients within the formation. As evident in Figure 7, the impact of accounting for vertical variations in temperature on the estimation of trapped CO₂ is

often more significant than assuming homogenous porosity or carbonate mineralogy. In this study, accounting for vertical differences in temperature resulted in up to a 10% simulated deviation in the sequestration efficiency between the homogeneous and heterogeneous models. It should be noted, however, that this observed deviation is formation dependent and reflects the unique properties of the model setup in this study.

5. Conclusions

The major goals of this work are to facilitate more rapid site assessment through an increased understanding of the formation properties at promising and active storage sites and assess potential CO₂ trapping, accounting for heterogeneities. Here, heterogeneity as it affects the field-scale sequestration of CO₂ is considered with the aim of providing a new perspective on the impact of aquifer property homogenization during typical site investigation resulting from limited data availability.

This work presents an aquifer evaluation framework which can provide insight towards a holistic understanding of aquifer storage potential to reduce greenhouse emissions of CO₂. Such an approach uses field-scale aquifer parameters that are typically obtained early in the site characterization or exploratory phase of a potential subsurface CO₂ storage project. Such an approach will aid in the sustainability of subsurface storage of CO₂ as a viable means of greenhouse gas reduction by helping to reduce the initial site screening in terms of both resource and time investment for an initial evaluation.

The aquifer data used for conducting the assessment were obtained through extensive literature review, the properties of active and promising sandstone aquifer storage sites were collected, and the range of promising aquifer properties was defined. Active storage sites show a high cluster density of data points falling in the 10–30% porosity and 10–1000 mD permeability range. In terms of mineralogy, all target sandstone formations are quartz-rich with calcite occurring as the most frequent carbonate mineral, present in 75% of formations. Clay minerals are commonly kaolinite or smectite/illite.

Based on observed variations in aquifer properties, homogeneous and heterogeneous models of CO₂ injection and subsequent evolution were developed to evaluate the impact of the spatial heterogeneity of promising formation properties on trapping in the formation. Deviations in the simulated extent and type of CO₂ trapping are observed in the simulation results over the fifty-year study period that comprised a ten-year injection phase followed by a forty-year monitoring phase.

During the injection phase, the homogenization of properties underestimates the trapping potential of the formation. Accounting for the temperature gradient has the largest effect on simulated CO₂ trapping, increasing the dissolved and mineralized CO₂. This may be explained by the fact that higher temperatures increase the kinetics of reactions. Systems with heterogeneous carbonate distributions and porosity also show an increased trapping potential compared to homogenous systems.

Post-injection, the temperature gradient still plays a dominant role, increasing the simulated amount of trapped CO₂. Homogenizing the formation porosity and carbonate mineralogy, however, increases the simulated amount of trapped CO₂.

Considering the implication of these observations on a typical storage site, we can see that understanding the temperature gradient of the target aquifer is a critical factor in estimating the sequestration efficiency. Fortunately, accurate estimation of the formation temperature gradient is more feasible than obtaining highly spatially resolved porosity and mineralogical composition data.

In general, the homogenization of the target aquifer porosity and mineralogy will give a conservative estimation of the geochemical potential of the target aquifer for CO₂ trapping given that the properties are within the defined, promising ranges noted here. If the properties have larger deviations than the favorable ranges defined here, greater variations in CO₂ trapping would be anticipated. While differences in simulated CO₂ trapping were observed, there was only a 10% deviation in CO₂ sequestration efficiency between the homogeneous and heterogenous model systems. As such, extensive investigation of the

variation in formation mineralogy and porosity at the core scale is not necessary to estimate the trapping potential of a formation given that the measured values are within the defined, promising range.

Supplementary Materials: The following supporting information can be downloaded at: <https://www.mdpi.com/article/10.3390/su16135515/s1>, Table S1: A table showing the percentage by volume and percentage by weight of the initial mineral composition of the Paluxy formation. The table also shows the specific gravity used for the conversion of the percentage by volume to percentage by weight; Table S2: The complete data set of the collected aquifer properties; Table S3: The complete data set of the aquifer mineralogies; Table S4: Base case mineral composition, mineral abundance, volume fraction, and reactive surface area of primary minerals [45], and reactive surface areas of secondary minerals [13]; Table S5: Fixed aquifer properties of the formation obtained from the literature. Geothermal gradient [48,49]. Hydrostatic gradient [47], liquid relative permeability and capillary pressure [52], and gaseous relative permeability [53]; Figure S1: A demonstration of the difference in the model setup for the study on the effect of aquifer porosity and carbonate mineralogy heterogeneity on sequestration efficiency. The heterogeneous model shows the random assignment of aquifer values for each grid cell. The homogeneous model has each grid cell assigned the average value of the heterogeneous model.

Author Contributions: Conceptualization, C.O.I. and L.E.B.; Methodology, C.O.I., F.C.O. and L.E.B.; Software, C.O.I.; Validation, C.O.I.; Formal analysis, C.O.I. and W.B.; Investigation, C.O.I. and W.B.; Resources, L.E.B.; Data curation, C.O.I., W.B., F.C.O. and L.E.B.; Writing—original draft, C.O.I.; Writing—review & editing, F.C.O. and L.E.B.; Visualization, C.O.I. and W.B.; Supervision, L.E.B.; Project administration, L.E.B.; Funding acquisition, L.E.B. All authors have read and agreed to the published version of the manuscript.

Funding: The authors Iloejesi and Beckingham acknowledge support from the Southeast Regional CO₂ Utilization and Storage Acceleration Partnership (SECARB-USA) project funded by the U.S. Department of Energy and cost-sharing partners under grant number FE0031830, managed by the Southern States Energy Board. Support is also acknowledged from Auburn University.

Data Availability Statement: The data presented in this study are available on request from the corresponding author.

Conflicts of Interest: The authors declare no conflict of interest.

References

1. Cuming, V.; Mills, L.; Strahan, D.; Boyle, R.; Stopforth, K.; Latimer, S.; Becker, L. Global Trends in Renewable Energy Investment. *Frankf. Sch. Financ. Manag.* **2015**, *5*.
2. Begum, R.A.; Sohag, K.; Abdullah, S.M.; Jaafar, M. CO₂ emissions, energy consumption, economic and population growth in Malaysia. *Renew. Sustain. Energy Rev.* **2015**, *41*, 594–601. [CrossRef]
3. Arnette, A.N. Renewable energy and carbon capture and sequestration for a reduced carbon energy plan: An optimization model. *Renew. Sustain. Energy Rev.* **2017**, *70*, 254–265. [CrossRef]
4. Edmonds, J.A.; Freund, P.F.; Dooley, J.J. *The Role of Carbon Management Technologies in Addressing Atmospheric Stabilization of Greenhouse Gases (No. PNWD-SA-5131)*; Pacific Northwest National Lab.: Richland, WA, USA, 2002.
5. Ciferno, J.P.; Fout, T.E.; Jones, A.P.; Murphy, J.T. Capturing carbon from existing coal-fired power plants. *Chem. Eng. Prog.* **2009**, *105*, 33.
6. Freund, P. Making deep reductions in CO₂ emissions from coal-fired power plant using capture and storage of CO₂. *Proc. Inst. Mech. Eng. Part A J. Power Energy* **2003**, *217*, 1–7. [CrossRef]
7. IPCC. Special Report on Carbon Dioxide Capture and Storage. Prepared by Working Group III of the Intergovernmental Panel on Climate Change. In *Environmental Science and Technology*; IPCC: Geneva, Switzerland, 2005.
8. NETL. *Carbon Storage Atlas: Fifth Edition*; U.S. Department of Energy-National Energy Technology Laboratory-Office of Fossil Energy: Albany, OR, USA, 2015.
9. Bentham, M.; Kirby, M. CO₂ storage in saline aquifers. *Oil Gas Sci. Technol. Rev. d'IFP Energies Nouv.* **2005**, *60*, 559–567. [CrossRef]
10. Doughty, C.; Freifeld, B.M.; Trautz, R.C. Site characterization for CO₂ geologic storage and vice versa: The Frio brine pilot, Texas, USA as a case study. *Environ. Geol.* **2008**, *54*, 1635–1656. [CrossRef]
11. Niemi, A.; Edlmann, K.; Carrera, J.; Juhlin, C.; Tatomir, A.; Ghergut, I.; Sauter, M.; Bensabat, J.; Fagerlund, F.; Cornet, F.H.; et al. Site characterization. In *Geological Storage of CO₂ in Deep Saline Formations*; Springer: Dordrecht, The Netherlands, 2017; pp. 309–380. [CrossRef]

12. Ennis-King, J.; Paterson, L. Role of convective mixing in the long-term storage of carbon dioxide in deep saline formations. In *SPE Annual Technical Conference and Exhibition*; OnePetro: Richardson, TX, USA, 2003.
13. Xu, T.; Apps, J.A.; Pruess, K. Numerical simulation of CO₂ disposal by mineral trapping in deep aquifers. *Appl. Geochem.* **2004**, *19*, 917–936. [[CrossRef](#)]
14. Riaz, A.; Hesse, M.; Tchelepi, H.A.; Orr, F.M. Onset of convection in a gravitationally unstable diffusive boundary layer in porous media. *J. Fluid Mech.* **2006**, *548*, 87–111. [[CrossRef](#)]
15. Deng, H.; Fitts, J.P.; Crandall, D.; McIntyre, D.; Peters, C.A. Alterations of fractures in carbonate rocks by CO₂-acidified brines. *Environ. Sci. Technol.* **2015**, *49*, 10226–10234. [[CrossRef](#)]
16. Hovorka, S.D.; Doughty, C.; Benson, S.M.; Pruess, K.; Knox, P.R. The impact of geological heterogeneity on CO₂ storage in brine formations: A case study from the Texas Gulf Coast. *Geol. Soc. Lond. Spéc. Publ.* **2004**, *233*, 147–163. [[CrossRef](#)]
17. Gaus, I.; Audigane, P.; André, L.; Lions, J.; Jacquemet, N.; Durst, P.; Czernichowski-Lauriol, I.; Azaroual, M. Geochemical and solute transport modelling for CO₂ storage, what to expect from it? *Int. J. Greenh. Gas Control.* **2008**, *2*, 605–625. [[CrossRef](#)]
18. Suekane, T.; Nobuso, T.; Hirai, S.; Kiyota, M. Geological storage of carbon dioxide by residual gas and solubility trapping. *Int. J. Greenh. Gas Control.* **2008**, *2*, 58–64. [[CrossRef](#)]
19. Benson, S.M.; Cole, D.R. CO₂ sequestration in deep sedimentary formations. *Elements* **2008**, *4*, 325–331. [[CrossRef](#)]
20. Kharaka, Y.K.; Cole, D.R. Geochemistry of geologic sequestration of carbon dioxide. *Front. Geochem. Contrib. Geochem. Study Earth* **2011**, *18*, 133–174. [[CrossRef](#)]
21. Zemke, K.; Liebscher, A.; Wandrey, M. Petrophysical analysis to investigate the effects of carbon dioxide storage in a subsurface saline aquifer at Ketzin, Germany (CO₂SINK). *Int. J. Greenh. Gas Control.* **2010**, *4*, 990–999. [[CrossRef](#)]
22. Morad, S.; Al-Ramadan, K.; Ketzer, J.M.; De Ros, L.F. The impact of diagenesis on the heterogeneity of sandstone reservoirs: A review of the role of depositional facies and sequence stratigraphy. *AAPG Bull.* **2010**, *94*, 1267–1309. [[CrossRef](#)]
23. Förster, A.; Norden, B.; Zinck-Jørgensen, K.; Frykman, P.; Kulenkampff, J.; Spangenberg, E.; Erzinger, J.; Zimmer, M.; Kopp, J.; Borm, G.; et al. Baseline characterization of the CO₂SINK geological storage site at Ketzin, Germany. *Environ. Geosci.* **2006**, *13*, 145–161. [[CrossRef](#)]
24. Juhlin, C.; Giese, R.; Zinck-Jørgensen, K.; Cosma, C.; Kazemeini, H.; Juhojuntti, N.; Lüth, S.; Norden, B.; Förster, A. 3D baseline seismics at Ketzin, Germany: The CO₂ SINK project. *Geophysics* **2007**, *72*, B121–B132. [[CrossRef](#)]
25. Wardlaw, N.C.; Taylor, R.P. Mercury capillary pressure curves and the interpretation of pore structure and capillary behaviour in reservoir rocks. *Bull. Can. Pet. Geol.* **1976**, *24*, 225–262.
26. Weber, K. Influence of common sedimentary structures on fluid flow in reservoir models. *J. Pet. Technol.* **1982**, *34*, 665–672. [[CrossRef](#)]
27. Lengler, U.; De Lucia, M.; Kühn, M. The impact of heterogeneity on the distribution of CO₂: Numerical simulation of CO₂ storage at Ketzin. *Int. J. Greenh. Gas Control.* **2010**, *4*, 1016–1025. [[CrossRef](#)]
28. Kumar, A.; Ozah, R.C.; Noh, M.H.; Pope, G.A.; Bryant, S.L.; Sepehrnoori, K.; Lake, L.W. Reservoir simulation of CO₂ storage in deep saline aquifers. *SPE J.* **2005**, *10*, 336–348. [[CrossRef](#)]
29. Ilojesi, C.O.; Zhang, S.; Beckingham, L.E. Impact of aquifer properties on the extent and timeline of CO₂ trapping. *Greenh. Gases Sci. Technol.* **2023**, *13*, 780–796. [[CrossRef](#)]
30. Hermanson, J.; Kirste, D. Representation of geological heterogeneities and their effects on mineral trapping during CO₂ storage using numerical modeling. *Procedia Earth Planet. Sci.* **2013**, *7*, 350–353. [[CrossRef](#)]
31. Shabani, B.; Lu, P.; Kammer, R.; Zhu, C. Effects of Hydrogeological Heterogeneity on CO₂ Migration and Mineral Trapping: 3D Reactive Transport Modeling of Geological CO₂ Storage in the Mt. Simon Sandstone, Indiana, USA. *Energies* **2022**, *15*, 2171. [[CrossRef](#)]
32. Tian, H.; Xu, T.; Zhu, H.; Yang, C.; Ding, F. Heterogeneity in mineral composition and its impact on the sealing capacity of caprock for a CO₂ geological storage site. *Comput. Geosci.* **2019**, *125*, 30–42. [[CrossRef](#)]
33. Hosa, A.; Esentia, M.; Stewart, J.; Haszeldine, S. Injection of CO₂ into saline formations: Benchmarking worldwide projects. *Chem. Eng. Res. Des.* **2011**, *89*, 1855–1864. [[CrossRef](#)]
34. Hommel, J.; Coltman, E.; Class, H. Porosity–permeability relations for evolving pore space: A review with a focus on (bio-)geochemically altered porous media. *Transp. Porous Media* **2018**, *124*, 589–629. [[CrossRef](#)]
35. Kumar, S.; Foroozesh, J.; Edlmann, K.; Rezk, M.G.; Lim, C.Y. A comprehensive review of value-added CO₂ sequestration in subsurface saline aquifers. *J. Nat. Gas Sci. Eng.* **2020**, *81*, 103437. [[CrossRef](#)]
36. Bachu, S. Review of CO₂ storage efficiency in deep saline aquifers. *Int. J. Greenh. Gas Control.* **2015**, *40*, 188–202. [[CrossRef](#)]
37. Goodman, A.; Hakala, A.; Bromhal, G.; Deel, D.; Rodosta, T.; Frailey, S.; Small, M.; Allen, D.; Romanov, V.; Fazio, J.; et al. U.S. DOE methodology for the development of geologic storage potential for carbon dioxide at the national and regional scale. *Int. J. Greenh. Gas Control.* **2011**, *5*, 952–965. [[CrossRef](#)]
38. Bentham, M. An assessment of carbon sequestration potential in the UK—Southern North Sea case study. *Nottm. Tyndall Cent. Clim. Change Res. Work. Pap. 85* **2006**.
39. Gunter, W.D.; Wiwehar, B.; Perkins, E.H. Aquifer disposal of CO₂-rich greenhouse gases: Extension of the time scale of experiment for CO₂-sequestering reactions by geochemical modelling. *Miner. Pet.* **1997**, *59*, 121–140. [[CrossRef](#)]
40. Cooper, C. A technical basis for carbon dioxide storage. *Energy Procedia* **2009**, *1*, 1727–1733. [[CrossRef](#)]

41. Tanase, D.; Sasaki, T.; Yoshii, T.; Motohashi, S.; Sawada, Y.; Aramaki, S.; Yamanouchi, Y.; Tanaka, T.; Ohkawa, S.; Inowaki, R. Tomakomai CCS demonstration project in Japan. *Energy Procedia* **2013**, *37*, 6571–6578. [[CrossRef](#)]
42. Xu, T.; Sonnenthal, E.; Spycher, N.; Zheng, L. *TOUGHREACT V3. 32 Reference Manual: A Parallel Simulation Program for Non-Isothermal Multiphase Geochemical Reactive Transport*; Lawrence Berkeley National Laboratory: Berkeley, CA, USA, 2017.
43. Pruess, K. ECO2N: A TOUGH2 fluid property module for mixtures of water, NaCl, and CO₂. Lawrence Berkeley National Laboratory: Berkeley, CA, USA, 2005.
44. Jalali, J.; Koperna, G.J.; Cyphers, S.; Riestenberg, D.; Esposito, R. Large Volume CO₂ Storage and Plume Management in the Southeastern US; Reservoir Characterization and Simulation. In Proceedings of the 15th Greenhouse Gas Control Technologies Conference, Abu Dhabi, United Arab Emirates, 16 March 2021; pp. 15–18. [[CrossRef](#)]
45. Qin, F.; Beckingham, L.E. Impact of image resolution on quantification of mineral abundances and accessible surface areas. *Chem. Geol.* **2019**, *523*, 31–41. [[CrossRef](#)]
46. Kuuskraa, V.; Koperna, G.; Riestenberg, D. *Commercial Development Plan (Deliverable 8.2) (No. DOE-SSEB-0029465-58)*; Southern States Energy Board: Peachtree Corners, GA, USA, 2020.
47. Pashin, J.C.; Hills, D.J.; Kopaska-Merkel, D.C.; McIntyre, M.R. *Geological Evaluation of the Potential for CO₂ Sequestration in Kemper County, Mississippi*; Final Report; Southern Company Research & Environmental Affairs: Birmingham, UK, 2008.
48. Warner, A.J. *Regional Geologic Framework of the Cretaceous, Offshore Mississippi*; Mississippi Department of Environmental Quality, Office of Geology: St. Jackson, MS, USA, 1993.
49. Nathenson, M.; Guffanti, M. Geothermal gradients in the conterminous United States. *J. Geophys. Res.* **1988**, *93*, 6437–6450. [[CrossRef](#)]
50. Tullis, J.; Yund, R.A. Grain growth kinetics of quartz and calcite aggregates. *J. Geol.* **1982**, *90*, 301–318. [[CrossRef](#)]
51. Mualem, Y. A new model for predicting the hydraulic conductivity of unsaturated porous media. *Water Resour. Res.* **1976**, *12*, 513–522. [[CrossRef](#)]
52. Van Genuchten, M.T. A Closed-form equation for predicting the hydraulic conductivity of unsaturated soils. *Soil Sci. Soc. Am. J.* **1980**, *44*, 892–898. [[CrossRef](#)]
53. Corey, A.T. The interrelation between gas and oil relative permeabilities. *Prod. Mon.* **1954**, *19*, 38–41.
54. Helgeson, H.C.; Kirkham, D.H. Theoretical prediction of the thermodynamic behavior of aqueous electrolytes at high pressures and temperatures; II, Debye-Huckel parameters for activity coefficients and relative partial molal properties. *Am. J. Sci.* **1974**, *274*, 1199–1261. [[CrossRef](#)]
55. Helgeson, H.C. Prediction of the thermodynamic properties of electrolytes at high pressures and temperatures. *Phys. Chem. Earth* **1981**, *13–14*, 133–177. [[CrossRef](#)]
56. Pearce, J.; Chadwick, A.; Kirby, G.; Holloway, S. The objectives and design of generic monitoring protocols for CO₂ storage. In Proceedings of the 8th International Conference on Greenhouse Gas Control (GHGT-8), Trondheim, Norway, 19–22 June 2006; Volume 6, p. 6.
57. Zhang, S.; DePaolo, D.J. Rates of CO₂ mineralization in geological carbon storage. *Accounts Chem. Res.* **2017**, *50*, 2075–2084. [[CrossRef](#)]
58. She, M.; Shou, J.; Shen, A.; Pan, L.; Hu, A.; Hu, Y. Experimental simulation of dissolution law and porosity evolution of carbonate rock. *Pet. Explor. Dev.* **2016**, *43*, 616–625. [[CrossRef](#)]
59. Smith, M.M.; Sholokhova, Y.; Hao, Y.; Carroll, S.A. CO₂-induced dissolution of low permeability carbonates. Part I: Characterization and experiments. *Adv. Water Resour.* **2013**, *62*, 370–387. [[CrossRef](#)]

Disclaimer/Publisher’s Note: The statements, opinions and data contained in all publications are solely those of the individual author(s) and contributor(s) and not of MDPI and/or the editor(s). MDPI and/or the editor(s) disclaim responsibility for any injury to people or property resulting from any ideas, methods, instructions or products referred to in the content.